

Search for Excited and Exotic Muons in the $\mu\gamma$ Decay Channel in $p\bar{p}$ Collisions at $\sqrt{s} = 1.96$ TeV

- A. Abulencia,²³ D. Acosta,¹⁷ J. Adelman,¹³ T. Affolder,¹⁰ T. Akimoto,⁵⁵ M.G. Albrow,¹⁶ D. Ambrose,¹⁶
 S. Amerio,⁴³ D. Amidei,³⁴ A. Anastassov,⁵² K. Anikeev,¹⁶ A. Annovi,¹⁸ J. Antos,¹ M. Aoki,⁵⁵ G. Apollinari,¹⁶
 J.-F. Arguin,³³ T. Arisawa,⁵⁷ A. Artikov,¹⁴ W. Ashmanskas,¹⁶ A. Attal,⁸ F. Azfar,⁴² P. Azzi-Bacchetta,⁴³
 P. Azzurri,⁴⁶ N. Bacchetta,⁴³ H. Bachacou,²⁸ W. Badgett,¹⁶ A. Barbaro-Galtieri,²⁸ V.E. Barnes,⁴⁸ B.A. Barnett,²⁴
 S. Baroiant,⁷ V. Bartsch,³⁰ G. Bauer,³² F. Bedeschi,⁴⁶ S. Behari,²⁴ S. Belforte,⁵⁴ G. Bellettini,⁴⁶ J. Bellinger,⁵⁹
 A. Belloni,³² E. Ben Haim,⁴⁴ D. Benjamin,¹⁵ A. Beretvas,¹⁶ J. Beringer,²⁸ T. Berry,²⁹ A. Bhatti,⁵⁰ M. Binkley,¹⁶
 D. Bisello,⁴³ R. E. Blair,² C. Blocker,⁶ B. Blumenfeld,²⁴ A. Bocci,¹⁵ A. Bodek,⁴⁹ V. Boisvert,⁴⁹ G. Bolla,⁴⁸
 A. Bolshov,³² D. Bortoletto,⁴⁸ J. Boudreau,⁴⁷ A. Boveia,¹⁰ B. Brau,¹⁰ C. Bromberg,³⁵ E. Brubaker,¹³ J. Budagov,¹⁴
 H.S. Budd,⁴⁹ S. Budd,²³ K. Burkett,¹⁶ G. Busetto,⁴³ P. Bussey,²⁰ K. L. Byrum,² S. Cabrera,¹⁵ M. Campanelli,¹⁹
 M. Campbell,³⁴ F. Canelli,⁸ A. Canepa,⁴⁸ D. Carlsmith,⁵⁹ R. Carosi,⁴⁶ S. Carron,¹⁵ B. Casal,¹¹ M. Casarsa,⁵⁴
 A. Castro,⁵ P. Catastini,⁴⁶ D. Cauz,⁵⁴ M. Cavalli-Sforza,³ A. Cerri,²⁸ L. Cerrito,⁴² S.H. Chang,²⁷ J. Chapman,³⁴
 Y.C. Chen,¹ M. Chertok,⁷ G. Chiarelli,⁴⁶ G. Chlachidze,¹⁴ F. Chlebana,¹⁶ I. Cho,²⁷ K. Cho,²⁷ D. Chokheli,¹⁴
 J.P. Chou,²¹ P.H. Chu,²³ S.H. Chuang,⁵⁹ K. Chung,¹² W.H. Chung,⁵⁹ Y.S. Chung,⁴⁹ M. Ciljak,⁴⁶ C.I. Ciobanu,²³
 M.A. Ciocci,⁴⁶ A. Clark,¹⁹ D. Clark,⁶ M. Coca,¹⁵ G. Compostella,⁴³ M.E. Convery,⁵⁰ J. Conway,⁷ B. Cooper,³⁰
 K. Copic,³⁴ M. Cordelli,¹⁸ G. Cortiana,⁴³ F. Crescioli,⁴⁶ A. Cruz,¹⁷ C. Cuena Almenar,⁷ J. Cuevas,¹¹
 R. Culbertson,¹⁶ D. Cyr,⁵⁹ S. DaRonco,⁴³ S. D'Auria,²⁰ M. D'Onofrio,³ D. Dagenhart,⁶ P. de Barbaro,⁴⁹
 S. De Cecco,⁵¹ A. Deisher,²⁸ G. De Lentdecker,⁴⁹ M. Dell'Orso,⁴⁶ F. Delli Paoli,⁴³ S. Demers,⁴⁹ L. Demortier,⁵⁰
 J. Deng,¹⁵ M. Deninno,⁵ D. De Pedis,⁵¹ P.F. Derwent,¹⁶ G.P. Di Giovanni,⁴⁴ B. Di Ruzza,⁵⁴ C. Dionisi,⁵¹
 J.R. Dittmann,⁴ P. DiTuro,⁵² C. Dörr,²⁵ S. Donati,⁴⁶ M. Donega,¹⁹ P. Dong,⁸ J. Donini,⁴³ T. Dorigo,⁴³
 S. Dube,⁵² K. Ebina,⁵⁷ J. Efron,³⁹ J. Ehlers,¹⁹ R. Erbacher,⁷ D. Errede,²³ S. Errede,²³ R. Eusebi,¹⁶ H.C. Fang,²⁸
 S. Farrington,²⁹ I. Fedorko,⁴⁶ W.T. Fedorko,¹³ R.G. Feild,⁶⁰ M. Feindt,²⁵ J.P. Fernandez,³¹ R. Field,¹⁷
 G. Flanagan,⁴⁸ L.R. Flores-Castillo,⁴⁷ A. Foland,²¹ S. Forrester,⁷ G.W. Foster,¹⁶ M. Franklin,²¹ J.C. Freeman,²⁸
 H. J. Frisch,¹³ I. Furic,¹³ M. Gallinaro,⁵⁰ J. Galyardt,¹² J.E. Garcia,⁴⁶ M. Garcia Sciveres,²⁸ A.F. Garfinkel,⁴⁸
 C. Gay,⁶⁰ H. Gerberich,²³ D. Gerdes,³⁴ S. Giagu,⁵¹ P. Giannetti,⁴⁶ A. Gibson,²⁸ K. Gibson,¹² C. Ginsburg,¹⁶
 N. Giokaris,¹⁴ K. Giolo,⁴⁸ M. Giordani,⁵⁴ P. Giromini,¹⁸ M. Giunta,⁴⁶ G. Giurgiu,¹² V. Glagolev,¹⁴ D. Glenzinski,¹⁶
 M. Gold,³⁷ N. Goldschmidt,³⁴ J. Goldstein,⁴² G. Gomez,¹¹ G. Gomez-Ceballos,¹¹ M. Goncharov,⁵³ O. González,³¹
 I. Gorelov,³⁷ A.T. Goshaw,¹⁵ Y. Gotra,⁴⁷ K. Goulianos,⁵⁰ A. Gresele,⁴³ M. Griffiths,²⁹ S. Grinstein,²¹
 C. Grossi-Pilcher,¹³ R.C. Group,¹⁷ U. Grundler,²³ J. Guimaraes da Costa,²¹ Z. Gunay-Unalan,³⁵ C. Haber,²⁸
 S.R. Hahn,¹⁶ K. Hahn,⁴⁵ E. Halkiadakis,⁵² A. Hamilton,³³ B.-Y. Han,⁴⁹ J.Y. Han,⁴⁹ R. Handler,⁵⁹ F. Happacher,¹⁸
 K. Hara,⁵⁵ M. Hare,⁵⁶ S. Harper,⁴² R.F. Harr,⁵⁸ R.M. Harris,¹⁶ K. Hatakeyama,⁵⁰ J. Hauser,⁸ C. Hays,¹⁵
 A. Heijboer,⁴⁵ B. Heinemann,²⁹ J. Heinrich,⁴⁵ M. Herndon,⁵⁹ D. Hidas,¹⁵ C.S. Hill,¹⁰ D. Hirschbuehl,²⁵ A. Hocker,¹⁶
 A. Holloway,²¹ S. Hou,¹ M. Houlden,²⁹ S.-C. Hsu,⁹ B.T. Huffman,⁴² R.E. Hughes,³⁹ J. Huston,³⁵ J. Incandela,¹⁰
 G. Introzzi,⁴⁶ M. Iori,⁵¹ Y. Ishizawa,⁵⁵ A. Ivanov,⁷ B. Iyutin,³² E. James,¹⁶ D. Jang,⁵² B. Jayatilaka,³⁴ D. Jeans,⁵¹
 H. Jensen,¹⁶ E.J. Jeon,²⁷ S. Jindariani,¹⁷ M. Jones,⁴⁸ K.K. Joo,²⁷ S.Y. Jun,¹² T.R. Junk,²³ T. Kamon,⁵³
 J. Kang,³⁴ P.E. Karchin,⁵⁸ Y. Kato,⁴¹ Y. Kemp,²⁵ R. Kephart,¹⁶ U. Kerzel,²⁵ V. Khotilovich,⁵³ B. Kilminster,³⁹
 D.H. Kim,²⁷ H.S. Kim,²⁷ J.E. Kim,²⁷ M.J. Kim,¹² S.B. Kim,²⁷ S.H. Kim,⁵⁵ Y.K. Kim,¹³ L. Kirsch,⁶ S. Klimenko,¹⁷
 M. Klute,³² B. Knuteson,³² B.R. Ko,¹⁵ H. Kobayashi,⁵⁵ K. Kondo,⁵⁷ D.J. Kong,²⁷ J. Konigsberg,¹⁷ A. Korytov,¹⁷
 A.V. Kotwal,¹⁵ A. Kovalev,⁴⁵ A. Kraan,⁴⁵ J. Kraus,²³ I. Kravchenko,³² M. Kreps,²⁵ J. Kroll,⁴⁵ N. Krumnack,⁴
 M. Kruse,¹⁵ V. Krutelyov,⁵³ S. E. Kuhlmann,² Y. Kusakabe,⁵⁷ S. Kwang,¹³ A.T. Laasanen,⁴⁸ S. Lai,³³ S. Lami,⁴⁶
 S. Lammel,¹⁶ M. Lancaster,³⁰ R.L. Lander,⁷ K. Lannon,³⁹ A. Lath,⁵² G. Latino,⁴⁶ I. Lazzizzera,⁴³ T. LeCompte,²
 J. Lee,⁴⁹ J. Lee,²⁷ Y.J. Lee,²⁷ S.W. Lee,⁵³ R. Lefèvre,³ N. Leonardo,³² S. Leone,⁴⁶ S. Levy,¹³ J.D. Lewis,¹⁶ C. Lin,⁶⁰
 C.S. Lin,¹⁶ M. Lindgren,¹⁶ E. Lipelis,⁹ T.M. Liss,²³ A. Lister,¹⁹ D.O. Litvintsev,¹⁶ T. Liu,¹⁶ N.S. Lockyer,⁴⁵
 A. Loginov,³⁶ M. Loretta,⁴³ P. Loverre,⁵¹ R.-S. Lu,¹ D. Lucchesi,⁴³ P. Lujan,²⁸ P. Lukens,¹⁶ G. Lungu,¹⁷ L. Lyons,⁴²
 J. Lys,²⁸ R. Lysak,¹ E. Lytken,⁴⁸ P. Mack,²⁵ D. MacQueen,³³ R. Madrak,¹⁶ K. Maeshima,¹⁶ T. Maki,²²
 P. Maksimovic,²⁴ S. Malde,⁴² G. Manca,²⁹ F. Margaroli,⁵ R. Marginean,¹⁶ C. Marino,²³ A. Martin,⁶⁰ V. Martin,³⁸
 M. Martínez,³ T. Maruyama,⁵⁵ P. Mastrandrea,⁵¹ H. Matsunaga,⁵⁵ M.E. Mattson,⁵⁸ R. Mazini,³³ P. Mazzanti,⁵
 K.S. McFarland,⁴⁹ P. McIntyre,⁵³ R. McNulty,²⁹ A. Mehta,²⁹ S. Menzemer,¹¹ A. Menzione,⁴⁶ P. Merkel,⁴⁸
 C. Mesropian,⁵⁰ A. Messina,⁵¹ M. von der Mey,⁸ T. Miao,¹⁶ N. Miladinovic,⁶ J. Miles,³² R. Miller,³⁵ J.S. Miller,³⁴

C. Mills,¹⁰ M. Milnik,²⁵ R. Miquel,²⁸ A. Mitra,¹ G. Mitselmakher,¹⁷ A. Miyamoto,²⁶ N. Moggi,⁵ B. Mohr,⁸ R. Moore,¹⁶ M. Morello,⁴⁶ P. Movilla Fernandez,²⁸ J. Mülmenstädt,²⁸ A. Mukherjee,¹⁶ Th. Muller,²⁵ R. Mumford,²⁴ P. Murat,¹⁶ J. Nachtman,¹⁶ J. Naganoma,⁵⁷ S. Nahn,³² I. Nakano,⁴⁰ A. Napier,⁵⁶ D. Naumov,³⁷ V. Necula,¹⁷ C. Neu,⁴⁵ M.S. Neubauer,⁹ J. Nielsen,²⁸ T. Nigmanov,⁴⁷ L. Nodulman,² O. Norniella,³ E. Nurse,³⁰ T. Ogawa,⁵⁷ S.H. Oh,¹⁵ Y.D. Oh,²⁷ T. Okusawa,⁴¹ R. Oldeman,²⁹ R. Orava,²² K. Osterberg,²² C. Pagliarone,⁴⁶ E. Palencia,¹¹ R. Paoletti,⁴⁶ V. Papadimitriou,¹⁶ A.A. Paramonov,¹³ B. Parks,³⁹ S. Pashapour,³³ J. Patrick,¹⁶ G. Pauletta,⁵⁴ M. Paulini,¹² C. Paus,³² D.E. Pellett,⁷ A. Penzo,⁵⁴ T.J. Phillips,¹⁵ G. Piacentino,⁴⁶ J. Piedra,⁴⁴ L. Pinera,¹⁷ K. Pitts,²³ C. Plager,⁸ L. Pondrom,⁵⁹ X. Portell,³ O. Poukhov,¹⁴ N. Pounder,⁴² F. Prakoshyn,¹⁴ A. Pronko,¹⁶ J. Proudfoot,² F. Ptahos,¹⁸ G. Punzi,⁴⁶ J. Pursley,²⁴ J. Rademacker,⁴² A. Rahaman,⁴⁷ A. Rakitin,³² S. Rappoccio,²¹ F. Ratnikov,⁵² B. Reisert,¹⁶ V. Rekovic,³⁷ N. van Remortel,²² P. Renton,⁴² M. Rescigno,⁵¹ S. Richter,²⁵ F. Rimondi,⁵ L. Ristori,⁴⁶ W.J. Robertson,¹⁵ A. Robson,²⁰ T. Rodrigo,¹¹ E. Rogers,²³ S. Rolli,⁵⁶ R. Roser,¹⁶ M. Rossi,⁵⁴ R. Rossin,¹⁷ C. Rott,⁴⁸ A. Ruiz,¹¹ J. Russ,¹² V. Rusu,¹³ H. Saarikko,²² S. Sabik,³³ A. Safonov,⁵³ W.K. Sakumoto,⁴⁹ G. Salamanna,⁵¹ O. Saltó,³ D. Saltzberg,⁸ C. Sanchez,³ L. Santi,⁵⁴ S. Sarkar,⁵¹ L. Sartori,⁴⁶ K. Sato,⁵⁵ P. Savard,³³ A. Savoy-Navarro,⁴⁴ T. Scheidle,²⁵ P. Schlabach,¹⁶ E.E. Schmidt,¹⁶ M.P. Schmidt,⁶⁰ M. Schmitt,³⁸ T. Schwarz,³⁴ L. Scodellaro,¹¹ A.L. Scott,¹⁰ A. Scribano,⁴⁶ F. Scuri,⁴⁶ A. Sedov,⁴⁸ S. Seidel,³⁷ Y. Seiya,⁴¹ A. Semenov,¹⁴ L. Sexton-Kennedy,¹⁶ I. Sfiligoi,¹⁸ M.D. Shapiro,²⁸ T. Shears,²⁹ P.F. Shepard,⁴⁷ D. Sherman,²¹ M. Shimojima,⁵⁵ M. Shochet,¹³ Y. Shon,⁵⁹ I. Shreyber,³⁶ A. Sidoti,⁴⁴ P. Sinervo,³³ A. Sisakyan,¹⁴ J. Sjolin,⁴² A. Skiba,²⁵ A.J. Slaughter,¹⁶ K. Sliwa,⁵⁶ J.R. Smith,⁷ F.D. Snider,¹⁶ R. Snihur,³³ M. Soderberg,³⁴ A. Soha,⁷ S. Somalwar,⁵² V. Sorin,³⁵ J. Spalding,¹⁶ M. Spezziga,¹⁶ F. Spinella,⁴⁶ T. Spreitzer,³³ P. Squillacioti,⁴⁶ M. Stanitzki,⁶⁰ A. Staveris-Polykalas,⁴⁶ R. St. Denis,²⁰ B. Stelzer,⁸ O. Stelzer-Chilton,⁴² D. Stentz,³⁸ J. Strologas,³⁷ D. Stuart,¹⁰ J.S. Suh,²⁷ A. Sukhanov,¹⁷ K. Sumorok,³² H. Sun,⁵⁶ T. Suzuki,⁵⁵ A. Taffard,²³ R. Takashima,⁴⁰ Y. Takeuchi,⁵⁵ K. Takikawa,⁵⁵ M. Tanaka,² R. Tanaka,⁴⁰ N. Tanimoto,⁴⁰ M. Tecchio,³⁴ P.K. Teng,¹ K. Terashi,⁵⁰ S. Tether,³² J. Thom,¹⁶ A.S. Thompson,²⁰ E. Thomson,⁴⁵ P. Tipton,⁴⁹ V. Tiwari,¹² S. Tkaczyk,¹⁶ D. Toback,⁵³ S. Tokar,¹⁴ K. Tollefson,³⁵ T. Tomura,⁵⁵ D. Tonelli,⁴⁶ M. Tönnesmann,³⁵ S. Torre,¹⁸ D. Torretta,¹⁶ S. Tourneur,⁴⁴ W. Trischuk,³³ R. Tsuchiya,⁵⁷ S. Tsuno,⁴⁰ N. Turini,⁴⁶ F. Ukegawa,⁵⁵ T. Unverhau,²⁰ S. Uozumi,⁵⁵ D. Usynin,⁴⁵ A. Vaiciulis,⁴⁹ S. Vallecorsa,¹⁹ A. Varganov,³⁴ E. Vataga,³⁷ G. Velev,¹⁶ G. Veramendi,²³ V. Vespremi,⁴⁸ R. Vidal,¹⁶ I. Vila,¹¹ R. Vilar,¹¹ T. Vine,³⁰ I. Vollrath,³³ I. Volobouev,²⁸ G. Volpi,⁴⁶ F. Würthwein,⁹ P. Wagner,⁵³ R. G. Wagner,² R.L. Wagner,¹⁶ W. Wagner,²⁵ R. Wallny,⁸ T. Walter,²⁵ Z. Wan,⁵² S.M. Wang,¹ A. Warburton,³³ S. Waschke,²⁰ D. Waters,³⁰ W.C. Wester III,¹⁶ B. Whitehouse,⁵⁶ D. Whiteson,⁴⁵ A.B. Wicklund,² E. Wicklund,¹⁶ G. Williams,³³ H.H. Williams,⁴⁵ P. Wilson,¹⁶ B.L. Winer,³⁹ P. Wittich,¹⁶ S. Wolbers,¹⁶ C. Wolfe,¹³ T. Wright,³⁴ X. Wu,¹⁹ S.M. Wynne,²⁹ A. Yagil,¹⁶ K. Yamamoto,⁴¹ J. Yamaoka,⁵² T. Yamashita,⁴⁰ C. Yang,⁶⁰ U.K. Yang,¹³ Y.C. Yang,²⁷ W.M. Yao,²⁸ G.P. Yeh,¹⁶ J. Yoh,¹⁶ K. Yorita,¹³ T. Yoshida,⁴¹ G.B. Yu,⁴⁹ I. Yu,²⁷ S.S. Yu,¹⁶ J.C. Yun,¹⁶ L. Zanello,⁵¹ A. Zanetti,⁵⁴ I. Zaw,²¹ F. Zetti,⁴⁶ X. Zhang,²³ J. Zhou,⁵² and S. Zucchelli⁵

(CDF Collaboration)

¹*Institute of Physics, Academia Sinica, Taipei, Taiwan 11529, Republic of China*

²*Argonne National Laboratory, Argonne, Illinois 60439*

³*Institut de Fisica d'Altes Energies, Universitat Autònoma de Barcelona, E-08193, Bellaterra (Barcelona), Spain*

⁴*Baylor University, Waco, Texas 76798*

⁵*Istituto Nazionale di Fisica Nucleare, University of Bologna, I-40127 Bologna, Italy*

⁶*Brandeis University, Waltham, Massachusetts 02254*

⁷*University of California, Davis, Davis, California 95616*

⁸*University of California, Los Angeles, Los Angeles, California 90024*

⁹*University of California, San Diego, La Jolla, California 92093*

¹⁰*University of California, Santa Barbara, Santa Barbara, California 93106*

¹¹*Instituto de Fisica de Cantabria, CSIC-University of Cantabria, 39005 Santander, Spain*

¹²*Carnegie Mellon University, Pittsburgh, PA 15213*

¹³*Enrico Fermi Institute, University of Chicago, Chicago, Illinois 60637*

¹⁴*Joint Institute for Nuclear Research, RU-141980 Dubna, Russia*

¹⁵*Duke University, Durham, North Carolina 27708*

¹⁶*Fermi National Accelerator Laboratory, Batavia, Illinois 60510*

¹⁷*University of Florida, Gainesville, Florida 32611*

¹⁸*Laboratori Nazionali di Frascati, Istituto Nazionale di Fisica Nucleare, I-00044 Frascati, Italy*

¹⁹*University of Geneva, CH-1211 Geneva 4, Switzerland*

²⁰*Glasgow University, Glasgow G12 8QQ, United Kingdom*

²¹*Harvard University, Cambridge, Massachusetts 02138*

- ²²*Division of High Energy Physics, Department of Physics,
University of Helsinki and Helsinki Institute of Physics, FIN-00014, Helsinki, Finland*
- ²³*University of Illinois, Urbana, Illinois 61801*
- ²⁴*The Johns Hopkins University, Baltimore, Maryland 21218*
- ²⁵*Institut für Experimentelle Kernphysik, Universität Karlsruhe, 76128 Karlsruhe, Germany*
- ²⁶*High Energy Accelerator Research Organization (KEK), Tsukuba, Ibaraki 305, Japan*
- ²⁷*Center for High Energy Physics: Kyungpook National University,
Taegu 702-701, Korea; Seoul National University, Seoul 151-742,
Korea; and SungKyunKwan University, Suwon 440-746, Korea*
- ²⁸*Ernest Orlando Lawrence Berkeley National Laboratory, Berkeley, California 94720*
- ²⁹*University of Liverpool, Liverpool L69 7ZE, United Kingdom*
- ³⁰*University College London, London WC1E 6BT, United Kingdom*
- ³¹*Centro de Investigaciones Energeticas Medioambientales y Tecnologicas, E-28040 Madrid, Spain*
- ³²*Massachusetts Institute of Technology, Cambridge, Massachusetts 02139*
- ³³*Institute of Particle Physics: McGill University, Montréal,
Canada H3A 2T8; and University of Toronto, Toronto, Canada M5S 1A7*
- ³⁴*University of Michigan, Ann Arbor, Michigan 48109*
- ³⁵*Michigan State University, East Lansing, Michigan 48824*
- ³⁶*Institution for Theoretical and Experimental Physics, ITEP, Moscow 117259, Russia*
- ³⁷*University of New Mexico, Albuquerque, New Mexico 87131*
- ³⁸*Northwestern University, Evanston, Illinois 60208*
- ³⁹*The Ohio State University, Columbus, Ohio 43210*
- ⁴⁰*Okayama University, Okayama 700-8530, Japan*
- ⁴¹*Osaka City University, Osaka 588, Japan*
- ⁴²*University of Oxford, Oxford OX1 3RH, United Kingdom*
- ⁴³*University of Padova, Istituto Nazionale di Fisica Nucleare,
Sezione di Padova-Trento, I-35131 Padova, Italy*
- ⁴⁴*LPNHE, Université Pierre et Marie Curie/IN2P3-CNRS, UMR7585, Paris, F-75252 France*
- ⁴⁵*University of Pennsylvania, Philadelphia, Pennsylvania 19104*
- ⁴⁶*Istituto Nazionale di Fisica Nucleare Pisa, Universities of Pisa,
Siena and Scuola Normale Superiore, I-56127 Pisa, Italy*
- ⁴⁷*University of Pittsburgh, Pittsburgh, Pennsylvania 15260*
- ⁴⁸*Purdue University, West Lafayette, Indiana 47907*
- ⁴⁹*University of Rochester, Rochester, New York 14627*
- ⁵⁰*The Rockefeller University, New York, New York 10021*
- ⁵¹*Istituto Nazionale di Fisica Nucleare, Sezione di Roma 1,
University of Rome “La Sapienza,” I-00185 Roma, Italy*
- ⁵²*Rutgers University, Piscataway, New Jersey 08855*
- ⁵³*Texas A&M University, College Station, Texas 77843*
- ⁵⁴*Istituto Nazionale di Fisica Nucleare, University of Trieste/ Udine, Italy*
- ⁵⁵*University of Tsukuba, Tsukuba, Ibaraki 305, Japan*
- ⁵⁶*Tufts University, Medford, Massachusetts 02155*
- ⁵⁷*Waseda University, Tokyo 169, Japan*
- ⁵⁸*Wayne State University, Detroit, Michigan 48201*
- ⁵⁹*University of Wisconsin, Madison, Wisconsin 53706*
- ⁶⁰*Yale University, New Haven, Connecticut 06520*

We present a search for excited and exotic muon states μ^* , conducted using an integrated luminosity of 371 pb^{-1} of data collected in $p\bar{p}$ collisions at $\sqrt{s} = 1.96 \text{ TeV}$ at the Tevatron with the CDF II detector. We search for associated production of $\mu\mu^*$ followed by the decay $\mu^* \rightarrow \mu\gamma$, resulting in the $\mu\mu\gamma$ final state. We compare the data to model predictions as a function of the mass of the excited muon M_{μ^*} , the compositeness energy scale Λ , and the gauge coupling factor f . No signal above the standard model expectation is observed in the $\mu\gamma$ mass spectrum. In the contact interaction model, we exclude $107 < M_{\mu^*} < 853 \text{ GeV}/c^2$ for $\Lambda = M_{\mu^*}$; in the gauge-mediated model, we exclude $100 < M_{\mu^*} < 410 \text{ GeV}/c^2$ for $f/\Lambda = 10^{-2} \text{ GeV}^{-1}$. These 95% confidence level exclusions extend previous limits and are the first hadron collider results on μ^* production in the gauge-mediated model.

PACS numbers: 12.60.Rc, 13.85.Qk, 12.60.-i, 14.60.Hi

In the standard model (SM) the quarks and leptons are treated as fundamental particles. Their generational structure and observed mass hierarchy motivate a model

of composite quarks and leptons consisting of fewer elementary particles than contained in the SM [1]. In this model, quarks and leptons are the lowest-energy bound

states of these hypothetical particles, and additional excited states exist near the compositeness energy scale Λ .

Exotic fermions are also predicted in the context of grand unified or string theories, in which the known forces are unified into a larger symmetry group [2]. In such models, additional fermions are predicted with properties similar to those of excited fermions.

At a $p\bar{p}$ collider, excited or exotic muon states could be observed through the reaction $q\bar{q} \rightarrow \mu^*\mu$. Excited muon production can be described using a contact interaction (CI) Lagrangian density [1]:

$$L = \frac{4\pi}{\Lambda^2} \bar{q}_L \gamma^\mu q_L \bar{M}_L \gamma_\mu \mu_L + h.c.,$$

where M_L represents the left-handed μ^* field. For exotic muon production, the relevant gauge-mediated (GM) Lagrangian density is [2]:

$$L = \frac{1}{2\Lambda} \bar{M}_R \sigma^{\mu\nu} \left[fg \frac{\vec{\tau}}{2} \cdot \vec{W}_{\mu\nu} + f' g' \frac{Y}{2} B_{\mu\nu} \right] \mu_L + h.c.,$$

where W and B are the $SU(2)_L$ and $U(1)_Y$ field strengths, g and g' are the respective electroweak couplings, and f and f' are phenomenological constants which are set equal to each other by convention to maximize the photonic decay branching ratio. For $f = f'$ ($f = -f'$), the relative μ^* branching ratios are $BR(\mu^* \rightarrow \mu\gamma) \approx 0.3$ (0), $BR(\mu^* \rightarrow \nu W) \approx 0.6$ (0.6), and $BR(\mu^* \rightarrow \mu Z) \approx 0.1$ (0.4) for $M_{\mu^*} > 200$ GeV/ c^2 . The $BR(\mu^* \rightarrow \mu\gamma)$ increases to 70% at $M_{\mu^*} = 100$ GeV/ c^2 for $f = f'$. We use these branching ratios for both the GM and CI production models [3].

In this Letter we describe a search for associated $\mu\mu^*$ production that extends existing μ^* mass limits. Prior searches for μ^* production have been performed by the LEP experiments, which have excluded μ^* with $M_{\mu^*} < 200$ GeV/ c^2 for $f/\Lambda > 10^{-2}$ GeV $^{-1}$ in the GM model [4]. The DØ experiment has excluded μ^* with $M_{\mu^*} < 688$ GeV/ c^2 for $\Lambda = M_{\mu^*}$ in a particular CI model [5].

We use 371 pb $^{-1}$ of data collected with the CDF II detector at the Fermilab Tevatron. The detector has been described in detail elsewhere [6]. Its magnetic spectrometer consists of silicon microstrip and drift chamber [7] tracking detectors. Surrounding this are central [8] ($|\eta| < 1$ [9]) and forward [10] ($|\eta| > 1.1$) electromagnetic (EM) and hadronic calorimeters. Embedded in the central EM calorimeter are wire and strip chambers [6] (used to measure the transverse shower profiles of photons) and a central preshower detector [6] (used for detecting photon conversions). Outside the calorimeters are CMUP ($|\eta| < 0.6$) and CMX ($0.6 < |\eta| < 1$) muon detectors [11]. The momentum resolution of beam-constrained drift-chamber tracks is $\delta p_T/p_T^2 \approx 0.05\%/(GeV/c)$. The electromagnetic energy resolution for the high-energy photons typical of μ^* decays is approximately 2.5%.

We analyze events passing the readout trigger requirement of one drift-chamber track with $p_T > 18$ GeV/ c [9]

matched to a reconstructed track segment in the muon chambers. In the offline analysis, we require two muon candidates identified by drift-chamber tracks with $p_T > 20$ GeV/ c and $|\eta| < 1$, which pass requirements on impact parameter and number of hits, have minimum-ionizing particle properties, and at least one of which has a matching muon chamber segment [12]. Both tracks must pass the calorimeter isolation requirement $I < 0.1$, where I is the ratio of the combined EM and hadronic calorimeter E_T surrounding the track in a cone of radius $R = \sqrt{(\Delta\eta)^2 + (\Delta\phi)^2} < 0.4$ [9] to the track p_T . In addition, both tracks must also pass the tracking isolation requirement $T < 0.1$, where T is the ratio of the summed p_T of tracks to the muon p_T , where the sum is taken over tracks in a cone of radius $R < 0.4$ around the muon direction. Finally, we reject cosmic rays based on tracking and track-timing information [13].

We select dimuon events that have a central or forward photon candidate with $E_T > 25$ GeV, $|\eta| < 2.8$, and $I < 0.1$, where calorimeter isolation is now defined relative to the photon. The photon energy is defined as the EM calorimeter energy in a 0.2×0.25 $\eta - \phi$ region, and its transverse component is determined by the vertex of the highest momentum muon with a matching muon chamber segment. Photon candidates are identified on the basis of their longitudinal and transverse calorimeter shower profiles. Central photon candidates require the sum p_T of charged particles within a cone of radius $R < 0.4$ around the photon direction to be less than 5 GeV + $0.005 \times E_T^\gamma$, where E_T^γ is the E_T of the photon, and no single charged particle within $R < 0.4$ to have $p_T > (1 + 0.005 \times E_T^\gamma/\text{GeV})$ GeV/ c . To suppress the initial-state radiation (ISR) $Z(\rightarrow \mu\mu)\gamma$ background, we reject events with dimuon invariant mass $m_{\mu\mu}$ in the range $81 - 101$ GeV/ c^2 .

A $Z \rightarrow \mu\mu$ sample is used to measure the efficiencies of the muon identification criteria and trigger. The efficiency of the calorimeter and tracking identification requirements is measured to be $(92.6 \pm 0.3_{\text{stat}})\%$. We measure the combined trigger and muon chamber matching efficiency to be $(79.3 \pm 1.0_{\text{stat}})\%$ for the CMUP and $(95.0 \pm 0.6_{\text{stat}})\%$ for the CMX.

The photon identification efficiency is extracted from a GEANT-based detector simulation [14]. Since the electromagnetic showers of electrons are similar to those of photons, we validate the simulated photon efficiency using a control sample of electrons from $Z \rightarrow ee$ events. The events are triggered and identified using one electron; the second electron is used to emulate the photon to determine the cut efficiencies for photons. In the central calorimeter, the emulated photon efficiency is $(79.0 \pm 0.5_{\text{stat}})\%$ in the data and $(77.0 \pm 0.6_{\text{stat}})\%$ in the simulation. The corresponding values in the forward calorimeter are $(89.0 \pm 0.6_{\text{stat}})\%$ in the data and $(89.6 \pm 0.6_{\text{stat}})\%$ in the simulation. These comparisons show that photon detection is well-modeled by the simu-

lation; the statistically significant differences are included in the systematic uncertainty.

The geometric acceptance and detector response are calculated with the GEANT detector simulation separately for the CI and GM models. We use the PYTHIA [15] generator for the CI model and the LANHEP [16] and COM-PHEP [17] programs to generate GM model events. The total signal acceptance (including identification efficiencies) for the CI model increases from 13% at $M_{\mu^*} = 100 \text{ GeV}/c^2$ to an asymptotic value of 21% for $M_{\mu^*} > 400 \text{ GeV}/c^2$. The acceptance for the GM model increases from 12% at $M_{\mu^*} = 100 \text{ GeV}/c^2$ to an asymptotic value of 23% for $M_{\mu^*} > 300 \text{ GeV}/c^2$. The relative systematic uncertainty on the acceptance is 3.1%, which is dominated by the uncertainty in the identification efficiency (2.2%) and simulation statistics (2.0%).

We compute the expected background contributions from the following sources: (1) $Z/\gamma^*(+\gamma) \rightarrow \mu\mu\gamma$, (2) $Z/\gamma^*(+\gamma) \rightarrow \tau\tau\gamma$, where the τ 's decay to muons, (3) $Z/\gamma^*(\rightarrow \mu\mu) + \text{jet}$, where the jet is misidentified as a photon, (4) $t(\rightarrow \mu\nu b) + \bar{t}(\rightarrow \mu\nu \bar{b})$, where a fermion radiates a photon, (5) $W(\rightarrow e\nu) + Z(\rightarrow \mu\mu)$, where the electron is misidentified as a photon, and (6) $Z(\rightarrow ee) + Z(\rightarrow \mu\mu)$, where one of the electrons is misidentified as a photon. Other backgrounds (≥ 3 jets, $W+ \geq 2$ jets, and $W\gamma+ \geq 1$ jet) were found to be negligible.

The $Z\gamma$, $t\bar{t}$, WZ and ZZ backgrounds are estimated using simulated events, with the ZGAMMA [18] generator for the $Z(\rightarrow \mu\mu)\gamma$ background and PYTHIA for the others. Systematic uncertainties on these background predictions arise due to integrated luminosity (6%) [19], parton distribution functions (PDFs) (5%), higher-order QCD corrections (5%) [20], acceptance (1%), and identification efficiencies (2%).

The $Z+\text{jet}$ background is estimated by weighting $Z+\text{jet}$ events from the data by an E_T -dependent jet $\rightarrow \gamma$ misidentification rate. The latter is measured using a jet-triggered data sample, correcting for the fraction of true prompt photons in the jet sample [3]. The prompt photon fraction is estimated using $\gamma \rightarrow ee$ conversions identified with the calorimeter preshower detector [21]. The jet $\rightarrow \gamma$ misidentification rate is applied as a function of E_T in the central calorimeter and as a function of E_T and η in the forward calorimeter.

We observe 17 signal candidates with a background prediction of 8.3 ± 0.9 , of which 8.1 ± 0.8 are expected from $Z\gamma$ production. The Poisson probability for the background to fluctuate up to the observation, or higher, is 0.8%. Investigating further, we find that 11 candidate events have a 3-body mass $m_{\mu\mu\gamma}$ in the $81\text{-}101 \text{ GeV}/c^2$ range, consistent with being final-state radiation (FSR) $Z \rightarrow \mu\mu\gamma$ events, to be compared to the FSR $Z \rightarrow \mu\mu\gamma$ prediction of 5.5 ± 0.5 events. Figure 1 and Table I show the $m_{\mu\gamma}$ and $m_{\mu\mu\gamma}$ distributions for the data and background.

To test our background prediction, we lower the mini-

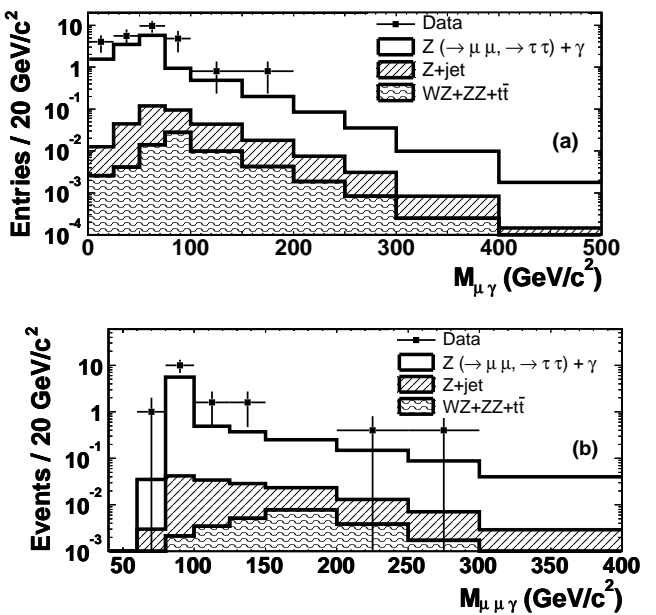


FIG. 1: The $\mu\gamma$ (a) and $\mu\mu\gamma$ (b) mass distributions for the data with background expectations. The total number of observed (expected) $\mu\mu\gamma$ entries is 17 (8.3 ± 0.9). Both $\mu\gamma$ combinations per event are included in (a).

num photon E_T to 15 GeV and observe 43 events with a prediction of 38.5 ± 4.0 events. The data show good agreement with expectation in this higher statistics sample, as shown in Figure 2. Additionally, we find consistency in the ISR $Z\gamma$ control region of $81 < m_{\mu\mu} < 101 \text{ GeV}/c^2$ and $25 < E_T^\gamma < 50 \text{ GeV}$, where we observe 5 events with a prediction of $7.2^{+1.2}_{-0.8}$ events. We conclude that our signal sample has an upward statistical fluctuation, dominantly in the number of FSR $Z \rightarrow \mu\mu\gamma$ events.

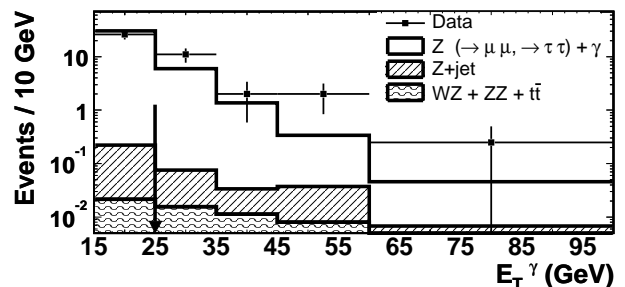


FIG. 2: The E_T^γ distributions for the data (43 events) and background (38.5 ± 4.0 events) expectations for $E_T^\gamma > 15 \text{ GeV}$. The arrow indicates the minimum E_T^γ required for this analysis.

For the μ^* resonance search, we scan the $m_{\mu\gamma}$ spectrum with a sliding window of width 3σ , where σ is the mass width predicted by the simulation. Over almost the

TABLE I: Comparison of data and integrated background predictions above a given cut on the invariant mass of all $\mu\gamma$ combinations (left) and on the $\mu\mu\gamma$ invariant mass (right).

$\mu\gamma$ combinations			Events		
$m_{\mu\gamma}$	Data	Background	$m_{\mu\mu\gamma}$	Data	Background
(GeV/c 2)			(GeV/c 2)		
> 0	34	16.6 ± 1.8	> 0	17	8.3 ± 0.9
> 50	22	10.4 ± 1.1	> 100	6	2.7 ± 0.3
> 100	4	2.1 ± 0.3	> 150	2	1.5 ± 0.2
> 150	2	0.89 ± 0.14	> 200	2	0.9 ± 0.1
> 200	0	0.37 ± 0.07	> 250	1	0.51 ± 0.09
			> 300	0	0.29 ± 0.06

entire model parameter space, σ is dominated by detector resolution. The tracker momentum scale and resolution, and the calorimeter energy scale and resolution, are tuned on the well-known $Z \rightarrow \mu\mu$ and $Z \rightarrow ee$ mass peaks [22], respectively. For $M_{\mu^*} = \Lambda$, the reconstructed $\mu\gamma$ mass resolution ranges from 9-90 GeV/c 2 for masses ranging from 200-800 GeV/c 2 .

We use a Bayesian [23] approach, with a flat prior on the signal cross section and gamma priors on acceptance and backgrounds, to set limits on the $\mu\mu^*$ production cross section as a function of M_{μ^*} [24]. The cross section limits are converted to M_{μ^*} limits by comparing them to the next-to-next-to-leading-order (NNLO) theoretical cross sections [20], computed using the MRST set of PDFs [25]. We use the CTEQ prescription [26] to calculate the cross section uncertainty due to PDFs, which varies from 5% ($M_{\mu^*} = 100$ GeV/c 2) to 20% ($M_{\mu^*} = 1$ TeV/c 2). Uncertainties on higher-order QCD corrections (7-13%) depend on M_{μ^*} and the production model.

Figure 3 shows the 95% confidence level (CL) upper limits on the experimental cross section \times branching ratio and the theoretical curves for $M_{\mu^*} = \Lambda/f$ ($M_{\mu^*} = \Lambda$) for the GM (CI) model. Masses below 221 GeV/c 2 (853 GeV/c 2) are excluded for the GM (CI) model for the case $M_{\mu^*} = \Lambda/f$ ($M_{\mu^*} = \Lambda$). Figure 4 shows the limits in the parameter space of f/Λ (M_{μ^*}/Λ) versus M_{μ^*} for the GM (CI) model. For both models, we lose sensitivity for $M_{\mu^*} < 100$ GeV/c 2 due to large backgrounds and loss of signal acceptance in this range. We note that our CI limit of $M_{\mu^*} > 853$ GeV/c 2 reduces to $M_{\mu^*} > 696$ GeV/c 2 if we use μ^* branching ratios that account for hypothetical CI decays, as assumed by the DØ collaboration [5].

In conclusion, we have presented a search for excited and exotic muons. In the GM model, we exclude $100 < M_{\mu^*} < 410$ GeV/c 2 for $f/\Lambda = 10^{-2}$ GeV $^{-1}$ at the 95% CL., which is the first GM result at a hadron collider and is substantially beyond previous limits [4]. We have also presented μ^* limits in the CI model as a function of M_{μ^*} and Λ , excluding $107 < M_{\mu^*} < 853$ GeV/c 2 for $\Lambda = M_{\mu^*}$. These limits complement our recent results of

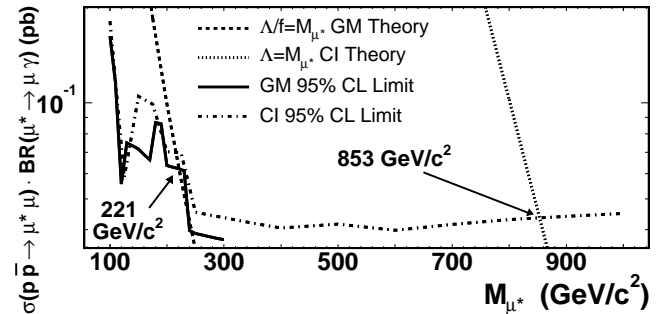


FIG. 3: The experimental cross section \times branching ratio limits at 95% CL for the CI (dashed-dotted line) and GM models (solid line), compared to the CI model prediction for $\Lambda = M_{\mu^*}$ (dotted line) and the GM model prediction for $\Lambda/f = M_{\mu^*}$ (dashed line). Also indicated are the mass values that are excluded by these data.

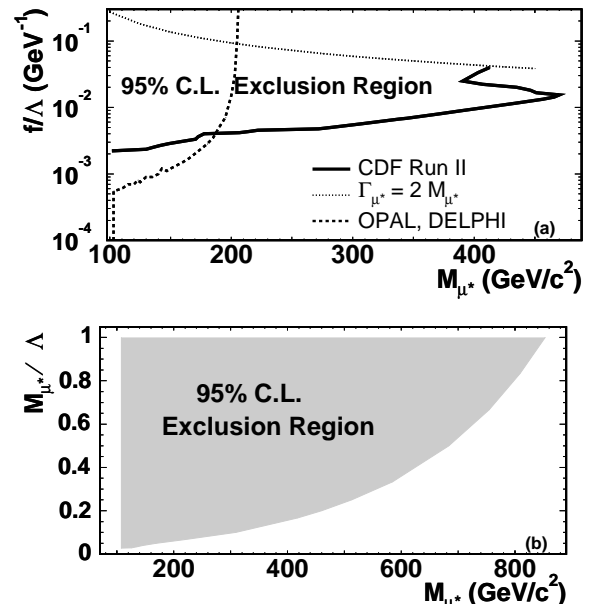


FIG. 4: The 2-D parameter space regions excluded by this analysis for (a) the GM model, along with the current world limits [4], and (b) the CI model. We do not consider the region $\Gamma_{\mu^*} > 2M_{\mu^*}$ where the total width is larger than the μ^* mass.

a search for excited and exotic electrons [3].

We are grateful to Alejandro Daleo for providing NNLO cross section calculations. We thank the Fermilab staff and the technical staffs of the participating institutions for their vital contributions. This work was supported by the U.S. Department of Energy and National Science Foundation; the Italian Istituto Nazionale

di Fisica Nucleare; the Ministry of Education, Culture, Sports, Science and Technology of Japan; the Natural Sciences and Engineering Research Council of Canada; the National Science Council of the Republic of China; the Swiss National Science Foundation; the A.P. Sloan Foundation; the Bundesministerium für Bildung und Forschung, Germany; the Korean Science and Engineering Foundation and the Korean Research Foundation; the Particle Physics and Astronomy Research Council and the Royal Society, UK; the Russian Foundation for Basic Research; the Comisión Interministerial de Ciencia y Tecnología, Spain; in part by the European Community's Human Potential Programme under contract HPRN-CT-2002-00292; and the Academy of Finland.

-
- [1] U. Baur, M. Spira, and P. M. Zerwas, Phys. Rev. D **42**, 815 (1990), and references therein.
 - [2] K. Hagiwara, S. Komamiya, and D. Zeppenfeld, Z. Phys. C **29**, 115 (1985), and references therein; E. Boos *et al.*, Phys. Rev. D **66**, 013011 (2002), and references therein.
 - [3] D. Acosta *et al.* (CDF Collaboration), Phys. Rev. Lett. **94**, 101802 (2005).
 - [4] G. Abbiendi *et al.* (OPAL Collaboration), Phys. Lett. B **544**, 57 (2002); J. Abdallah *et al.* (DELPHI Collaboration), Eur. Phys. J. C **46**, 277 (2006).
 - [5] V. Abazov *et al.* (DØ Collaboration), Phys. Rev. D **73**, 111102 (2006).
 - [6] D. Acosta *et al.* (CDF Collaboration), Phys. Rev. D **71**, 032001 (2005).
 - [7] T. Affolder *et al.*, Nucl. Instrum. Methods Res. A **526**, 249 (2004).
 - [8] F. Abe *et al.* (CDF Collaboration), Nucl. Instrum. Methods Res. A **271**, 387 (1988).
 - [9] CDF uses a cylindrical coordinate system in which ϕ is the azimuthal angle, r is the radius from the nominal beamline, and $+z$ points in the direction of the proton beam and is zero at the center of the detector. The pseudorapidity is defined as $\eta = -\ln[\tan(\theta/2)]$, where θ is the polar angle with respect to the z axis. Calorimeter energy (track momentum) measured transverse to the beam is denoted as E_T (p_T).
 - [10] M. G. Albrow *et al.*, Nucl. Instrum. Methods Res. A **480**, 524 (2002); **431**, 104 (1999); P. de Barbaro *et al.*, IEEE Trans. Nucl. Sci. **42**, 510 (1995).
 - [11] G. Ascoli *et al.*, Nucl. Instrum. Methods Res. A **268**, 33 (1988).
 - [12] A. Abulencia *et al.* (CDF Collaboration), hep-ex/0508029 (2005), submitted to Phys. Rev. D.
 - [13] A. Kotwal, H. Gerberich, and C. Hays, Nucl. Instrum. Methods Res. A **480**, 110 (2003).
 - [14] R. Brun and F. Carminati, CERN Program Library Long Writeup, W5013, 1993 (unpublished), version 3.15.
 - [15] T. Sjöstrand, Comput. Phys. Commun. **82**, 74 (1994), version 6.127. We divide the μ^* production cross-section calculated by PYTHIA v6.127 by a factor of 2, to be consistent with PYTHIA v6.211, as described in the PYTHIA release notes.
 - [16] A. V. Semenov, hep-ph/0208011 (2002); A. V. Semenov, Comput. Phys. Commun. **115**, 124 (1998).
 - [17] A. Pukhov *et al.*, hep-ph/9908288 (1999); E. E. Boos *et al.*, hep-ph/9503280 (1995).
 - [18] U. Baur and E. Berger, Phys. Rev. D **47**, 4889 (1993).
 - [19] S. Klimenko, J. Konigsberg, and T.M. Liss, FERMILAB-FN-0741 (2003); D. Acosta *et al.*, Nucl. Instrum. Methods Res. A **494**, 57 (2002).
 - [20] U. Baur, T. Han, and J. Ohnemus, Phys. Rev. D **57**, 2823 (1998); R. Hamberg, W. L. Van Neerven, and T. Matsuura, Nucl. Phys. B **359**, 343 (1991), [Erratum-ibid. B **644**, 403 (2002)]; R. V. Harlander and W. B. Kilgore, Phys. Rev. Lett. **88**, 201801 (2002); A. Daleo, private communication. We use NNLO cross sections evaluated with the MRST set of PDFs.
 - [21] H. Gerberich, Ph.D. Thesis, Duke University, UMI-31-78699, 157-179 (2004).
 - [22] S. Eidelman *et al.* (Particle Data Group), Physics Letters B **592**, 1 (2004).
 - [23] J. Heinrich *et al.*, physics/0409129 (2004); K. Hagiwara *et al.*, Phys. Rev. D **66**, 010001 (2002), section 31.
 - [24] An event is considered a μ^* candidate for a given mass hypothesis if at least one $\mu\gamma$ combination has a reconstructed mass in the sliding mass window.
 - [25] A. D. Martin *et al.*, Eur. Phys. J. C **4**, 463 (1998); Eur. Phys. J. C **23**, 73 (2002).
 - [26] J. Pumplin *et al.*, J. High Energy Phys. **0207**, 012 (2002).